J. Synchrotron Rad. (1997). 4, 180–184

On the Off-Bragg Reflectivity Enhancement in Dynamical Multiple Diffraction of X-rays by an $In_{0.5}Ga_{0.5}P/GaAs$ Heteroepitaxial Structure

M. V. Koval'chuk, A. Ya. Kreines, L. V. Samoilova and A. M. Mel'nikov

A. V. Shubnikov Institute of Crystallography, Russian Academy of Sciences, Leninskii Prospekt 59, 117333 Moscow, Russia. E-mail: kreines@radio-msu.net

(Received 30 August 1996; accepted 27 January 1997)

The effect of dynamical interactions between reflections involved in 000/111/220 multiple diffraction by an $In_{0.5}Ga_{0.5}P/GaAs$ heteroepitaxial structure was observed, which significantly increases the intensity of the (111) reflection in the region of the total (220) reflection from the substrate during Renninger-like scanning. The amplitude of the peak is roughly five times as great as the peak of detoured excitation for ideal GaAs. Possible applications of the observed feature in synchrotron-radiation-based studies are discussed.

Keywords: dynamical diffraction; multiple diffraction; heterostructures.

1. Introduction

Interference effects in the dynamical scattering of X-rays by crystals provide a basis for a wide range of methods for investigating the structure of crystals and thin films (double- and triple-crystal diffractometry, various modifications of the X-ray standing-wave method, diffraction under total external reflection conditions). All the above-mentioned methods are based on the use of two-beam diffraction, where the electromagnetic field inside a crystal can be represented as a superposition of two strong waves, one incident and one diffracted. In reciprocal space, this corresponds to the situation where one reciprocal lattice node (in addition to the zero node) is located near the Ewald sphere.

The dynamical effects become much more versatile when three or more reciprocal lattice nodes fall in the vicinity of the Ewald sphere (Chang, 1981). In this situation, three or more strong beams exist within the crystal; their superposition gives rise to a spatially modulated wavefield that is periodical simultaneously in two or three dimensions and reproduces the periodicity of the crystal lattice. The important feature of multiple-diffraction experiments is that the reflection intensities depend on the phases of the reflections involved.

For a long time, application of multiple diffraction in the Bragg geometry has been connected with measuring the dependence of the intensity of weak reflections on the angle of azimuthal rotation (Renninger scanning) (for example, Colella, 1974). Here, the *Umweganregung* effect is observed near multiple-diffraction points that scatter the incident beam in the direction of the reference reflection **h** *via* the crystallographic planes corresponding to the additional reflection **g** and coupling reflection **g–h**.

Recently, the Renninger effect was successfully used to determine directly the phases of structure factors in inorganic (Schmidt & Colella, 1985) and organic (Shen & Colella, 1988; Chang, King, Huang & Gao, 1991) crystals and even in quasicrystals (Lee, Colella & Chapman, 1993). Shen (1986) showed that the shape of the tails of the Renninger peak can be described based on the second Born approximation and is linearly related to the phase of triplet invariant of the reflections involved in scattering. This approach has been used in the virtual scattering method (Chapman, Yoder & Colella, 1981), in which the shape of the tails of the Renninger peaks is analyzed in the vicinity of the multiple-diffraction point.

Multibeam diffraction has also proved useful in studies of heterostructures. Simultaneous diffraction from several crystallographic planes allows information on relative changes in interplanar distances for several crystallographic directions to be obtained in one experiment. In some cases, the effect of hybrid multiple diffraction (Isherwood, 1981; Morelhao, Cardoso, Sasaki & Carvalho, 1991), which is characteristic of multilayer systems and forms additional reflections coupled by successive Bragg–Laue and Laue–Bragg–Laue reflections in different layers of a multilayer system, is highly sensitive to tangential (with respect to the interface) components of the displacement fields (Isherwood, 1981; Chang *et al.*, 1991).

All the above-described studies were performed in layouts characterized by low angular resolution. Until recently, high-precision studies of the multiple-diffraction effects on highly perfect single crystals and crystalline structures (superlattices, heterostructures, nanostructures) met strong experimental problems: first, the incident beam should be collimated in two planes, and second, the angular dependences of the reflectivity should be measured with high angular resolution (to a few arcsec).

Wide adoption of intense sources of synchrotron radiation changed the situation; the fulfilment of high-

© 1997 International Union of Crystallography
Printed in Great Britain – all rights reserved

ISSN 0909-0495 © 1997

resolution multiple-diffraction measurements became possible. For example, the X-ray standing-wave method with fluorescence (Greiser & Materlik, 1987) and photoelectron (Kazimirov, Koval'chuk, Kohn *et al.*, 1993) registration was recently implemented in a three-beam configuration. The anomalous transmission enhancement under conditions of symmetrical six-beam Laue diffraction was studied diffractometrically (Kazimirov, Koval'chuk & Kohn, 1993). The high-precision investigations of multiple diffraction were performed on single crystals (see the review by Kazimirov, Koval'chuk & Kohn, 1994).

In our previous studies it has been shown that the excitation on the 'tail' of the reflectivity curve for the simultaneous reflection can be described within perturbation theory provided the curve is measured at a certain angular distance from the exact Bragg position. The shape of this excitation is directly related to the phase of the structure amplitude of the strong main reflection (in a similar fashion to the secondary radiation yield in the X-ray standing-wave method). This fact makes it possible to study the structure of thin subsurface layers in single crystals (Koval'chuk, Kazimirov, Kohn, Kreines & Samoilova, 1996). It seems of interest to use this scheme in studies of a more complex system, namely, a crystal with a thin film.

The aim of this work was to study the interference effects on an $In_{0.5}Ga_{0.5}P$/GaAs heteroepitaxial structure under conditions of multiple diffraction close to a three-beam Bragg point and analyze their possible applications in investigations of the film and interface structure.

2. Experimental

We studied an $In_{0.5}Ga_{0.5}P$/GaAs(111) heterostructure produced by liquid-phase epitaxy. The thickness of the film was 0.6 µm. For reference, we present the scattering parameters for the sample in Table 1. The μt value for the film was 0.3. For comparison, we also measured the appropriate dependences of the reflectivity for a perfect symmetrically cut GaAs(111) crystal.

We measured the reflection coefficient for the sample as a function of the angle of azimuthal rotation, φ, at a fixed value of the rocking angle, θ, near the exact Bragg position for multiple diffraction 000/111/220 for the substrate. In the measurements, performed on the instrument described by Kreines, Koval'chuk, Shilin, Shishkov & Kazimirov (1995), we used the characteristic Cu $K\alpha_1$ radiation. The incident beam was collimated in two mutually perpendicular planes by using two symmetrically cut Ge(111) crystals, one flat, the other channel-cut, placed on goniometers with mutually perpendicular axes. The flat crystal, struck first by the beam, was mounted on a goniometer with a vertical axis of rotation; the channel-cut crystal was placed on a goniometer with a horizontal axis of rotation. The X-ray optical layout collimated the beam to 15 arcsec in the horizontal plane and 12 arcsec in the vertical plane. The instrumental function was determined from the FWHM

Table 1
Parameters of X-ray scattering by GaAs and $In_{0.5}Ga_{0.5}P$.

μ is the linear absorption coefficient and L_{ex} is the extinction length.

	$1/\mu$ (µm)	$L_{ex(111)}$ (µm)	$L_{ex(220)}$ (µm)
GaAs	29.2	0.673	0.725
$In_{0.5}Ga_{0.5}P$	17.7	0.775	0.941

(full width at half maximum) values for the symmetrical reflection (111) and the skew-asymmetrical reflection (220) measured far from the exact multiple-diffraction point. The intensity of the incident beam was ~4000 counts s^{-1}, which was sufficient to observe the effect.

The angular position of the sample was adjusted as follows. First the sample was rotated around the θ axis so that the sample surface formed the symmetrical reflection Bragg angle with the incident beam. After adjustment of the conventional two-beam reflection, the second scintillation detector was installed near the sample at a position where it would be struck by the beam reflected from the (220) plane at the exact three-beam point. Then we azimuthally rotated the sample (around the axis perpendicular to the sample surface; in the following this angle will be denoted by φ) until the intensity of the beam recorded by the second detector increased, which showed that the exact multiple-diffraction position had been approached. Then we readjusted the (111) reflection, followed by the (220) reflection again; this procedure was repeated until the intensities of the beams recorded by both detectors reached

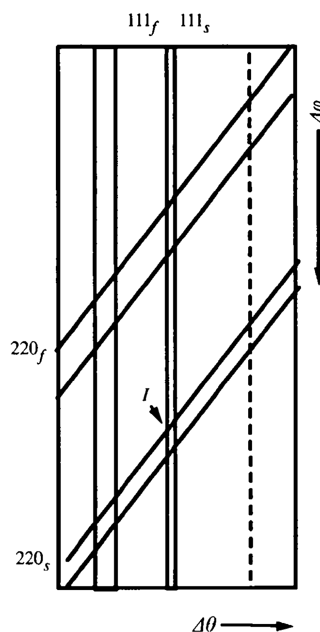

Figure 1
The θ–φ diagram illustrating the experimental geometry (see text for details). The angular scan performed is indicated by the dashed line. Subscripts f and s correspond to the film and substrate, respectively.

the maximal value, which indicated that we had adjusted the sample to the exact multiple-diffraction position. After this, the sample could be rotated from the exact multiple-diffraction position either by θ, in order to measure the reflectivity as a function of φ at constant θ (Renninger-like scheme), or by φ, in order to measure the reflectivity as a function of θ at constant φ.

The geometry of the experiment is illustrated by the θ–φ diagram (Kohn & Samoilova, 1992) presented in Fig. 1. The coordinate axes of this diagram represent the deviation of the sample position from exact diffraction conditions. The regions of total reflection from the film and the substrate are represented as bands in the diagram. The vertical bands correspond to the (111) reflection and the inclined bands correspond to the (220) reflection. The initial position of the sample after adjustment corresponds to angular region *I* (the exact multiple-diffraction position for the substrate). The Renninger-like scanning is schematically shown by the dashed line. In our experiments, the θ angular deviation from the exact Bragg position was 90 arcsec. This angle was maintained constant as we rotated the sample by φ.

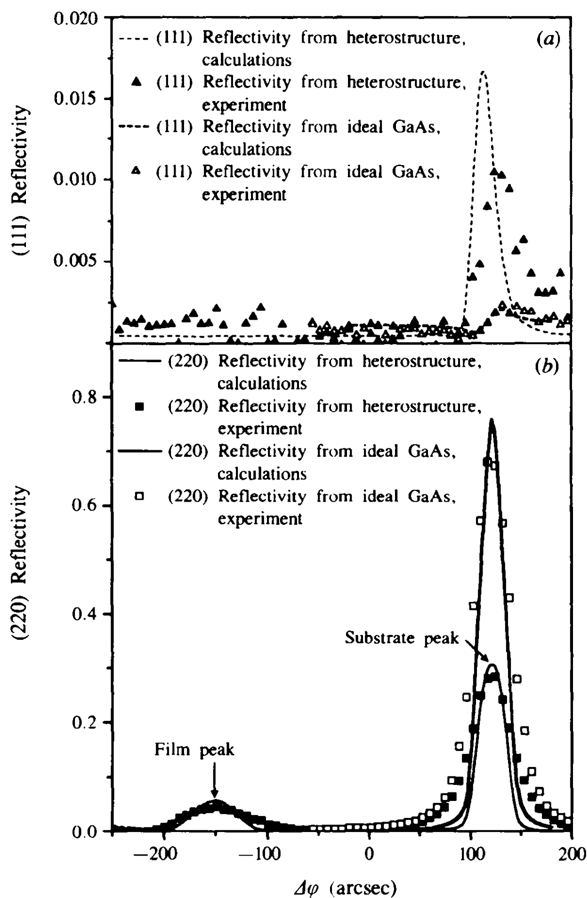

Figure 2
The experimental and calculated dependences of (*a*) (111)- and (*b*) (220)-reflectivity on φ near the multiple-diffraction point for 000/111/220 Cu $K\alpha_1$ diffraction on the GaAs (111) and $In_{0.5}Ga_{0.5}P$/GaAs (111) samples. The θ deviation from the exact (111) position is 90 arcsec. The points indicate the experimental results and the lines represent the calculations.

3. Results and discussion

The measured dependences of the reflectivity on φ are presented in Fig. 2. The dependence of the reflectivity for an ideal GaAs crystal exhibits a conventional phase-sensitive feature, similar to those measured in experiments with Si single crystals (Koval'chuk *et al.*, 1996). For the heterostructure the shape of the curve is cardinally different. In the region of the strong (220) reflection from the substrate, the intensity of the (111) reflection is drastically increased. The amplitude of this feature is approximately five times higher than that for the ideal crystal. This enhancement cannot be attributed to the refraction-induced change in the incidence angle for the substrate because the shift in this angle is $\sim$10 arcsec, which cannot result in a fivefold increase in the reflectivity for 90 arcsec angular displacement from the exact Bragg conditions.

In the same figure we present the results of numerical calculations. It is seen that the experimental curve for the ideal crystal agrees well with the calculation results. The curves for the heterostructure, in turn, exhibit qualitative agreement between theory and experiment. The calculations for the heterostructure were performed under the assumption that the film features no tetragonal distortions. The lattice mismatch between the film and the substrate, which is required for the calculations, was determined from the angular distance between the peaks for the substrate and the film on the two-beam (111) curve; it was found to be 2×10^{-3}. The curves presented were obtained by convoluting the intrinsic angular dependences of the reflectivity on the φ value with

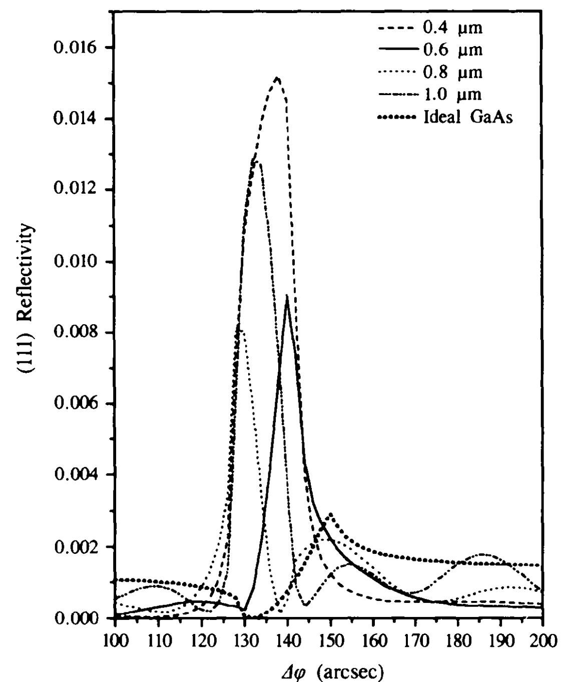

Figure 3
Plane-wave φ-scanning curves for the $In_{0.5}Ga_{0.5}P$/GaAs (111) samples with different film thicknesses measured under the same conditions as those shown in Fig. 2. Only the (111) reflectivity curves are presented.

the previously determined instrumental function. The best agreement between experiment and curves calculated by the algorithm presented by Kohn & Samoilova (1992) was achieved for Debye–Waller factor values of 0.7 for the film and 0.9 for the substrate. For ideal GaAs, the value of the Debye–Waller factor was 0.95.

In the first approximation, multiple diffraction of X-rays on a heterostructure can be represented as a superposition of three processes: (i) scattering from the substrate, (ii) scattering from the film, and (iii) scattering in the film of the beam diffracted from the substrate. Our estimations (a detailed theoretical investigation will be published elsewhere) show that the intensity of the (111)-diffracted beam is controlled by processes (i) and (iii). The latter can be thought of as 'hybrid diffraction' (Isherwood, 1981), the $(\bar{1}\bar{1}1)$ Laue diffraction (by the reciprocal lattice vector corresponding to the coupling reflection) in the film of the beam, that has been Bragg-reflected by the (220) vector in the substrate. The direction of such a double-diffracted beam almost coincides with that formed by diffraction of the incident beam by the (111) reciprocal lattice vector. This effect is of dynamical nature, which is confirmed by Fig. 3, where we present the intrinsic reflection curves calculated for the samples with films of different thickness. The change in the curve shape is strongest when the film thickness is approximately equal to the extinction length of the (111) reflection.

The discrepancy between the theoretical and the experimental curves may be attributed, for instance, to the tetragonal distortions in the film and the low crystal perfection of the film.

The intensity of the incident beam only allowed us to study relatively thick films. It would be much more interesting, however, to investigate the described effect in much thinner films; this may only be performed using synchrotron radiation.

The observed enhancement of the reflectivity has certain advantages as a tool for characterization of thinner films compared with traditional two-beam diffraction methods. In fact, it can be seen from Fig. 3 that the amplitude of the feature depends non-monitonically on the film thickness, whereas the amplitude of the film peak in two-beam curves is known to decrease monotonically with the film thickness. Furthermore, the two-beam peaks for the film broaden with decreasing film thickness, whereas the angular width of the observed feature remains constant (it is determined by the width of the strong multiple reflection). For thin films it is very difficult to find the blurred two-beam diffraction peak from the film on the background of the slowly decreasing tail of the substrate peak (for this purpose one may have to use strongly asymmetrical diffraction schemes or some other special conditions); the multiple-diffraction feature is much more observable. This is confirmed by Fig. 4, where we present the calculated feature for a 30 nm-thick film. The feature for this film has a magnitude comparable with and a shape easily distinguishable from that for ideal GaAs. At the same time, the calculated two-beam curves for ideal GaAs and ideal GaAs with a 30 nm $In_{0.5}Ga_{0.5}P$ film show very little difference, and no pronounced film peak can be observed.

Moreover, the studies of the observed feature in thin films would allow one to obtain information on the structure of the interface between the film and the substrate. Fig. 4 illustrates the calculated effect of the interface on the (111) reflection curve measured in our geometry. The calculations were performed for a hypothetical heterostructure consisting of a thick ideal GaAs crystal with a 30 nm $In_{0.5}Ga_{0.5}P$ film. The figure displays the curves calculated for structures characterized by different bond lengths at the interface in comparison with the intrinsic curve for an ideal GaAs crystal. To model the variation in the bond length at the interface, we artificially set the displacement of the lowermost atomic plane of the film with respect to the periodic system of the reflecting crystallographic planes in the substrate to be 0, $d_{111}/4$ and $d_{111}/2$ and calculated the resulting curves.

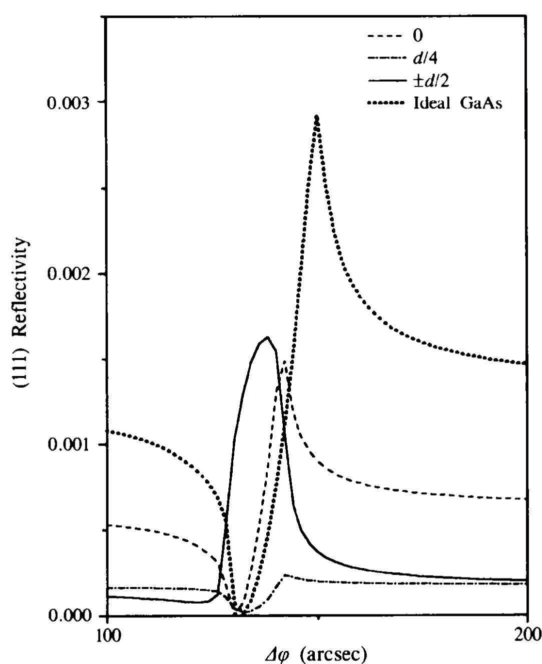

Figure 4
The calculated effect of the interface structure in $In_{0.5}Ga_{0.5}P/GaAs$ (111) samples with a 30 nm-thick film on the (111) Renninger-like scans. Different curves correspond to different bond lengths at the interface measured in fractions of the (111) interplanar distance.

The authors are grateful to the Russian Foundation for Basic Research for the support of this study.

References

Chang, S. L. (1981). *Acta Cryst.* **A37**, 876–879.

Chang, S. L., King, H. E., Huang, M.-T. & Gao, Y. (1991). *Phys. Rev. Lett.* **67**(22), 3113.

Chapman, L. D., Yoder, D. R. & Colella, R. (**1981**). *Phys. Rev. Lett.* **46**, 1578.

Colella, R. (1974). *Acta Cryst.* **A30**, 413–423.

Greiser, N. & Materlik, G. (1987). *Z. Phys. B Condens. Matter*, **66**, 83.

Isherwood, B. J. (1981). *J. Cryst. Growth*, **54**, 449.

Kazimirov, A. Yu., Koval'chuk, M. V. & Kohn, V. G. (1993). *Europhys. Lett.* **24**(3), 211–216.

Kazimirov, A. Yu., Koval'chuk, M. V. & Kohn, V. G. (1994). *Cryst. Rep.* **39**(2), 216–226.

Kazimirov, A. Yu., Koval'chuk, M. V., Kohn, V. G., Kharitonov, I. Yu., Samoilova, L. V., Ishikawa, T., Kikuta, S. & Hirano, K. (1993). *Phys. Status Solidi A*, **135**, 507–511.

Kohn, V. G. & Samoilova, L. V. (1992). *Phys. Status Solidi A*, **133**, 9–16.

Koval'chuk, M. V., Kazimirov, A. Yu., Kohn, V. G., Kreines, A. Ya. & Samoilova, L. V. (1996). *Physica B*, **221**, 445–450.

Kreines, A. Ya., Koval'chuk, M. V., Shilin, Yu. N., Shishkov, V. A. & Kazimirov, A. Yu. (1995). *SRI'95 Conference Abstracts*, Argonne, pp. 114–115.

Lee, H., Colella, R. & Chapman, L. D. (1993). *Acta Cryst.* A**49**, 600–605.

Morelhao, S., Cardoso, L., Sasaki, J. & Carvalho, M. (1991). *J. Appl. Phys.* **70**(5), 2589–2593.

Schmidt, M. C. & Colella, R. (1985). *Phys. Rev. Lett.* **55**, 715–717.

Shen, Q. (1986). *Acta Cryst.* A**42**, 525–533.

Shen, Q. & Colella, R. (1988). *Acta Cryst.* A**44**, 17–21.